

Quantum restricted Boltzmann machine universal for quantum computation

Yusen Wu^{1,2,3}, **Chunyan Wei**¹, **Sujuan Qin**¹, **Qiaoyan Wen**¹, and ***Fei Gao**^{1,3}

¹*State Key Laboratory of Networking and Switching Technology, Beijing University of Posts and Telecommunications, Beijing, 100876, China*

²*State Key Laboratory of Cryptology, P.O. Box 5159, Beijing, 100878, China*

³*Center for Quantum Computing, Peng Cheng Laboratory, Shenzhen 518055, China*

**gao@bupt.edu.cn*

The challenge posed by the many-body problem in quantum physics originates from the difficulty of describing the nontrivial correlations encoded in the many-body wave functions with high complexity. Quantum neural network provides a powerful tool to represent the large-scale wave function, which has aroused widespread concern in the quantum superiority era. A significant open problem is what exactly the representational power boundary of the single-layer quantum neural network is. In this paper, we design a 2-local Hamiltonian and then give a kind of Quantum Restricted Boltzmann Machine (QRBM, i.e. single-layer quantum neural network) based on it. The proposed QRBM has the following two salient features. (1) It is proved universal for implementing quantum computation tasks. (2) It can be efficiently implemented on the Noisy Intermediate-Scale Quantum (NISQ) devices. We successfully utilize the proposed QRBM to compute the wave functions for the notable cases of physical interest including the ground state as well as the Gibbs state (thermal state) of molecules on the superconducting quantum chip. The experimental results illustrate the proposed QRBM can compute the above wave functions with an acceptable error.

The wave function is an important object in quantum physics and is difficult to be characterized in the classical world. Actually, wave function encodes all of the information of a complex molecule on a quantum state which needs an extremely large-scale space to characterize. Generally, the scale of the space increases exponentially with the size of the physical system, therefore a large-scale wave function with complex correlations among the subsystems needs too enormous resources to depict with a classical computer. To address the above problem, Feynman proposed the idea that one can utilize a quantum computer to simulate complex wave functions [1], then some quantum algorithms for solving many-body problems of interacting fermions were developed [2, 3]. These algorithms depend on a “good” initial state that has a large overlap with the target state [5], and this is followed by the phase estimation algorithm. Noting that though these algorithms can produce an extremely accurate energy for quantum chemistry and quantum material, they apply stringent requirements on the coherence of the quantum hardware devices which are inaccessible with current technology.

To reduce the coherence requirements on the quantum devices, classical-quantum hybrid algorithms were delivered. This kind of algorithms involve minimizing a cost function that depends on the parameters of a quantum gate sequence. Cost evaluation occurs on the quantum computer, with speed-up over classical evaluation, and the classical computer utilizes this cost information to adjust the parameters of the ansatz with the help of suitable classical optimization algorithms. As one of the most representative classical-quantum hybrid algorithms, the Variational Quantum Eigensolver (VQE) utilizes Ritz’s variational principle to prepare approximations to the ground state and its energy [4]. However, the efficiency of VQEs is limited by the number of parameters that scales quartically with the number of spin orbitals that are considered in the single- and double- excitation approximation. To improve the VQE algorithm, the hardware-efficient trial states were introduced, which are composed by the single-qubit Euler rotation part and the entanglement part [5], and the hardware-efficient ansatz can be efficiently implemented on the Noisy Intermediate-Scale Quantum (NISQ) devices.

The quantum neural network is a significant ansatz in simulating many-body systems [6]. In fact, the neural network is a powerful tool to interpret complex correlations in multiple-variable functions or probability distributions in the classical world. Numerical experiment suggests that the single layer neural network, i.e.

the Restricted Boltzmann Machine (RBM), provides a good solution to several many-body systems, such as the transverse-field Ising model and the antiferromagnetic Heisenberg model [6]. However, the representation power of the RBM is not sufficient for implementing the universal quantum computation tasks. Duan et al. [8] analyzed the representational power of the RBM, and indicated that the RBM cannot characterize some of the quantum states, such as the projected entangled pair states and quantum enhanced feature states [7, 8].

Afterwards, researchers proposed the Quantum Restricted Boltzmann Machines (QRBM) to efficiently simulate some many-body systems. In 2018, Xia et al. [11] introduced a series of single-qubit rotation to construct a marginal state of the QRBM, which provides a good solution on simulating the Hydrogen molecule as well as the Water molecule. Zhang et al. [12] proposed a variational quantum algorithm to efficiently train the QRBM, where the proposed algorithm reduced the required ancillary qubits. Recently, Carleo et al. [13] presented an extension of quantum neural network to model interacting fermionic problems. The previous works show outstanding performance in some notable cases of physical interest that are difficult for classical RBM. These results suggest the QRBM has stronger representational power compared with the RBM, and this conjecture is also verified in some quantum machine learning algorithms [7, 16, 17, 18, 19, 20, 21]. However, as pointed out by Roger G. Melko et al. [22], whether the QRBM can implement universal quantum computation tasks is still a significant open problem.

In this paper, we utilize a 2-local Hamiltonian to induce a kind of QRBM, which we call 2-Local QRBM (2L-QRBM). Different from the previous QRBM, the 2L-QRBM has connections between visible nodes. Specifically, our model has two salient features. (1) It is proved universal for implementing quantum computation tasks. To do this, we provide two theorems to construct a map between the 2L-QRBM and the quantum circuit model. Given an arbitrary quantum state $|\alpha\rangle$ that is produced by a quantum circuit, the proof begins at indicating that the state $|\alpha\rangle$ can be encoded as the ground state of a 2-local Hamiltonian \mathcal{H} (Theorem 1). Then we propose how to construct a 2L-QRBM whose corresponding marginal state $|\Phi\rangle$ is $\mathcal{O}(\epsilon)$ close to the ground state of \mathcal{H} (Theorem 2), where ϵ is the approximation error. It implies that, compared with the classical RBM which cannot simulate an arbitrary quantum state [8], QRBM illustrates the advantages in terms of the representative power. (2) The proposed 2L-QRBM can be efficiently transformed to a quantum circuit and then be easily implemented on the NISQ devices. Based on this advantage, we validate the accuracy of the proposed 2L-QRBM by studying the Hydrogen molecule as well as the Water molecule on the quantum simulator. And we also utilize 2L-QRBM to compute the Gibbs states of Haldane chains on the superconducting devices. The power of the 2L-QRBM is demonstrated, obtaining state-of-art accuracy in computing ground states and Gibbs states.

Results

The construction of 2L-QRBM. The QRBM are commonly constituted by one visible layer of N nodes $\mathbf{v} = \{v_i\}_{i=1}^N$ corresponding to the physical spin variables in a chosen basis, and a single hidden layer of M auxiliary nodes $\mathbf{h} = \{h_j\}_{j=1}^M$. To satisfy the representation power for implementing universal computation tasks, we design a $2^{(N+M)} \times 2^{(N+M)}$ bipartite Hamiltonian:

$$\mathcal{H}_{RBM}(\boldsymbol{\theta}) = \sum_{i=1}^N \sum_{t \in \{x, y, z\}} b_i^t v_i^t + \sum_{j=1}^M m_j h_j^z + \sum_{i=1}^N \sum_{j=1}^M W_{ij} v_i^z h_j^z + \sum_{s=1}^{N-1} \sum_{k=s+1}^N \sum_{t \in \{x, y, z\}} K_{sk}^t v_s^t v_k^t \quad (1)$$

to depict the potential energy on each nodes and the interactions between \mathbf{v} and \mathbf{h} . The notation v_i^t represents the Pauli operator $\sigma_i^t (t \in \{x, y, z\})$ defined on the i -th visible nodes, h_j^z denotes the Pauli operator σ_j^z on the j -th hidden node, and the Boltzmann parameter $\boldsymbol{\theta} = \{b_i^t, m_j, W_{ij}, K_{sk}^t\} \in \mathcal{R}^{poly(N)}$. The schematic diagram of 2L-QRBM is illustrated as Fig.1. In the Hamiltonian $\mathcal{H}_{RBM}(\boldsymbol{\theta})$, the first two terms indicate the energy operators defined on the visible qubits and hidden qubits, respectively. The third term represents the connections between the visible layer and the hidden layer, and the final term expresses the intersections between visible nodes. Note that the Hamiltonian $\mathcal{H}_{RBM}(\boldsymbol{\theta})$ does not contain the intersections between hidden nodes, therefore $\mathcal{H}_{RBM}(\boldsymbol{\theta})$ can induce a QRBM [9].

The 2L-QRBM can be created with a two-step approach. First, entangle $N + M$ qubits (including all

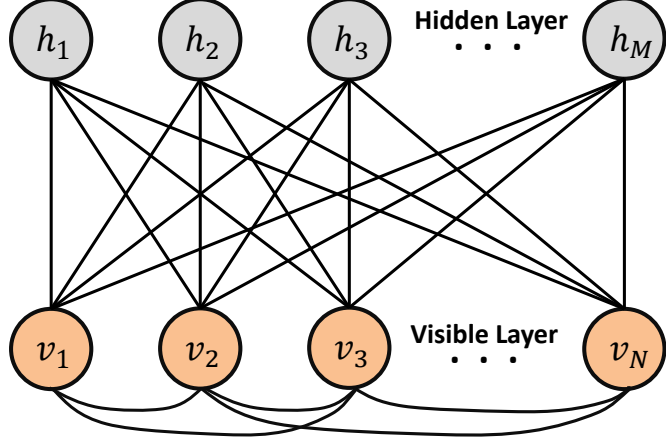


Figure 1: 2L-QRBM induced by the Hamiltonian $\mathcal{H}_{RBM}(\theta)$. The 2L-QRBM has N visible nodes as well as M hidden nodes. In the Hamiltonian $\mathcal{H}_{RBM}(\theta)$, the first two terms indicate the energy operators $b_i^t v_i^t$ and $m_j h_j^z$ defined on the visible qubits and hidden qubits, respectively. The third term $W_{ij} v_i^z h_j^z$ represents the connections between the visible layer and the hidden layer, and the final term $K_{sk}^t v_s^t v_k^t$ expresses the intersections between visible nodes.

visible and hidden nodes of a QRBM architecture) according to

$$|\Psi_{vh}(\theta)\rangle = \frac{e^{\mathcal{H}_{RBM}(\theta)} H^{\otimes(N+M)} |0\rangle_{vh}^{\otimes(N+M)}}{\sqrt{\langle +|^{\otimes(N+M)} e^{2\mathcal{H}_{RBM}(\theta)} |+\rangle^{\otimes(N+M)}}}, \quad (2)$$

where the notation H is the Hadamard gate, $|+\rangle = \frac{1}{\sqrt{2}}(|0\rangle + |1\rangle)$, and the notation $(\langle +|^{\otimes(N+M)} e^{2\mathcal{H}_{RBM}(\theta)} |+\rangle^{\otimes(N+M)})^{-1/2}$ is a normalization factor that guarantees the amplitudes in $|\Psi_{vh}(\theta)\rangle$ being normalized. Note that $e^{\mathcal{H}_{RBM}(\theta)}$ is a non-unitary operator that is difficult to be implemented on the quantum computer in general. To solve this problem, we will propose a method to transform $e^{\mathcal{H}_{RBM}(\theta)}$ into a series of fundamental quantum gates so that one can implement it efficiently on the NISQ devices.

Second, once the wave function $|\Psi_{vh}(\theta)\rangle$ is generated, all the hidden nodes (qubits) will be post-measured by $|+\rangle$. The measurement should be executed several times until all the hidden nodes (qubits) are projected onto the state $|+\rangle$. After that, the 2L-QRBM trial state can be expressed as

$$|\Psi_v(\theta)\rangle = \frac{\langle +|_h^{\otimes M} |\Psi_{vh}(\theta)\rangle}{\sqrt{\langle \Psi_{vh}(\theta) | P_+^{(h)} |\Psi_{vh}(\theta) \rangle}} = \frac{1}{N_v} \sum_h e^{\mathcal{H}_{RBM}(\theta, h)} |+\rangle^{\otimes N}, \quad (3)$$

in which $P_+^{(h)} = (|+\rangle\langle+|)_1 \otimes \dots \otimes (|+\rangle\langle+|)_M$ is the measurement operator, and N_v is the normalization factor. The notation $e^{\mathcal{H}_{RBM}(\theta, h)}$ is an operator acting on the visible nodes, which is composed by substituting the Pauli operator h_j^z to a binary value $(1 - 2h_j) \in \{-1, +1\}$ and $h_j \in |\mathbf{h}\rangle = |h_1 h_2 \dots h_M\rangle$. The wave function $|\Psi_v(\theta)\rangle$ is defined as the 2L-QRBM trial state. One can utilize the trial state $|\Psi_v(\theta)\rangle$ to approximate the target wave function of the realistic physical system.

2L-QRBM is universal for quantum computation. It is well known that the quantum circuit model is universal for quantum computation task, that is there exist sets of gates acting on a constant number of qubits that can efficiently simulate a quantum Turing machine [29]. In 2005, Aharonov et al. [25] proved that the Adiabatic Quantum Computation (AQC) is also universal for quantum computation, that is the AQC can simulate the output of any quantum circuit in the polynomial time. Here, we prove that the 2L-QRBM is universal for implementing quantum computation tasks in a similar way.

Theorem. *The QRBM induced by the Hamiltonian $\mathcal{H}_{RBM}(\boldsymbol{\theta})$ (Eq.(1)) can implement universal quantum computation tasks, that is, for an arbitrary quantum circuit whose output is denoted as $|\alpha\rangle$ and an arbitrary positive value ϵ , there exists a QRBM trial state $|\Psi_v(\boldsymbol{\theta})\rangle$ that is $\mathcal{O}(\epsilon)$ close to $|\alpha\rangle$.*

Detailed proof can refer to Methods, and we here give a brief overview. We first indicate that the output state $|\alpha\rangle$ of an arbitrary quantum circuit can be encoded and embedded into the ground state of a 2-local Hamiltonian \mathcal{H} (see Theorem 1 in Methods), then prove that there exists a 2L-QRBM trial state $|\Psi_v(\boldsymbol{\theta})\rangle$ converging towards the ground state of \mathcal{H} (see Theorem 3 in Methods). This naturally constructs a bridge between the quantum circuit model and the QRBM. The elaborate proof is illustrated as follows.

For the classic RBM, increasing the number of hidden nodes can enhance the representation power of the model. To illustrate the representation power of QRBMs, we consider the worst case for 2L-QRBMs, that is, there is only one hidden node ($M = 1$) and the potential energy on the hidden node equals to zero ($m_1 = 0$). In this case, the 2L-QRBMs trial state degrades to $|\Psi_v(\boldsymbol{\theta})\rangle = c^{-1/2} \langle + |_h \exp(\mathcal{H}_{RBM}(\boldsymbol{\theta}, m_j = 0)) | + \rangle_h | + \rangle_v^{\otimes N}$, where c is the normalized factor. Introducing a small constant t_0 provided by the Trotter theorem, $|\Psi_v(\boldsymbol{\theta})\rangle$ can be further expressed as

$$c^{-1/2} \bigotimes_{i=1}^N \langle + |_h \exp(W_{i,1} v_i^z h_1^z) | + \rangle_h \exp(\mathcal{H}_{ax}(\tilde{\boldsymbol{\theta}})) | + \rangle_v^{\otimes N} + \mathcal{O}(t_0^2) \quad (4)$$

when the norm of each parameters $(W_{ij}, b_i^t, K_{sk}^t)$ are bounded by $\mathcal{O}(t_0)$, and the auxiliary Hamiltonian $\mathcal{H}_{ax}(\tilde{\boldsymbol{\theta}}) = \sum_{i=1}^N \sum_{t \in \{x,y,z\}} b_i^t v_i^t + \sum_{s=1}^{N-1} \sum_{k=s+1}^N \sum_{t \in \{x,y,z\}} K_{sk}^t v_s^t v_k^t$. Noting that the expectation of $\exp(W_{i,1} v_i^z h_1^z)$ under the state $|+\rangle$ equals to $\frac{1}{2}(e^{W_{i,1}} + e^{-W_{i,1}}) \cdot I$, 2L-QRBMs trial state can be further expressed as

$$|\Psi_v(\boldsymbol{\theta})\rangle = \frac{c^{-1/2}}{2^N} \prod_{i=1}^N (e^{W_{i,1}} + e^{-W_{i,1}}) \exp(\mathcal{H}_{ax}(\tilde{\boldsymbol{\theta}})) | + \rangle_v^{\otimes N}, \quad (5)$$

where $\tilde{\boldsymbol{\theta}} = \{b_i^t, K_{sk}^t\} \in \mathcal{R}^{poly(N)}$ is the analogue of the Boltzmann parameter.

Since the trial state $|\Psi_v(\boldsymbol{\theta})\rangle$ can be rewritten as Eq.(5), we aim to find out the relationship between an arbitrary state $|\alpha(l)\rangle$ that is produced by a quantum circuit and the trial state $|\Psi_v(\boldsymbol{\theta})\rangle$. According to the Theorem 1 (see Methods), given a l -layer quantum circuit that outputs the quantum state $|\alpha(l)\rangle$ ($1 \leq l \leq L$) and an arbitrary small value ϵ , there exists a 2-local Hamiltonian \mathcal{H} whose ground state is $\mathcal{O}(\epsilon)$ close to the target quantum state $|\alpha(l)\rangle$. Based on the Theorem 2, the construction of $\mathcal{H}_{ax}(\tilde{\boldsymbol{\theta}})$ promises it can approximate any 2-local Hamiltonian in the ground state subspace (see Methods), then there exists a 2-local Hamiltonian $\mathcal{H}_{ax}(\tilde{\boldsymbol{\theta}})$ whose ground state is extremely close to that of \mathcal{H} . That is to say, the ground state of $\mathcal{H}_{ax}(\tilde{\boldsymbol{\theta}})$ is $\mathcal{O}(\epsilon)$ close to the target $|\alpha(l)\rangle$. Up to now, utilizing QRBMs trial state to compute the state $|\alpha(l)\rangle$ transforms into approximating the ground state of $\mathcal{H}_{ax}(\tilde{\boldsymbol{\theta}})$. Next we propose how to construct a 2L-QRBMs trial state to approximate it.

According to the Theorem 3 (see Methods), the ground state of $\mathcal{H}_{ax}(\tilde{\boldsymbol{\theta}})$ can be approximated by a 2L-QRBMs trial state $|\Psi_v(\boldsymbol{\theta}^*)\rangle$ with Boltzmann parameters $\boldsymbol{\theta}^* = \{m_j, W_{i1}, b_i^t, K_{sk}^t\} = \{0, \ln(e^{\lambda^* \tau/n} + \sqrt{e^{2\lambda^* \tau/n} - 1}), -\tau \tilde{\boldsymbol{\theta}}\}$. That is to say, the ground state of $\mathcal{H}_{ax}(\tilde{\boldsymbol{\theta}})$ is bounded by the representation boundary of the QRBMs trial state.

Now we complete the whole proof. The target quantum state $|\alpha(l)\rangle$ can be easily encoded as the ground state of the Hamiltonian $\mathcal{H}_{ax}(\tilde{\boldsymbol{\theta}})$, then one can construct a 2L-QRBMs trial state $|\Psi_v(\boldsymbol{\theta}^*)\rangle$ to approximate the ground state of $\mathcal{H}_{ax}(\tilde{\boldsymbol{\theta}})$. The bridge is naturally constructed between the QRBMs model and the quantum circuit model, therefore the 2L-QRBMs trial state can implement the universal quantum computation task. The elaborate proofs of the relevant theorems are proposed in Methods.

Quantum advantages of 2L-QRBMs. In this section, we describe the essence on quantum advantages of 2L-QRBMs in the field of representation power. Actually, the classical analogue of 2L-QRBMs is the RBM with connections of any two visible nodes, and its marginal distribution can be described as $\Psi(\mathbf{v}) = \sum_{\mathbf{h}} e^{E(\mathbf{v}, \mathbf{h})}$, where $E(\mathbf{v}, \mathbf{h}) = \sum_i b_i v_i + \sum_j m_j h_j + \sum_{ij} W_{ij} v_i h_j + \sum_{i,j} K_{ij} v_i v_j$. One may ask whether the representation advantages come from the inner-connection visible layer, however, the enhanced representational power is provided by the quantum mechanism. An interpretable example is that the classical RBM with an inner-connection visible layer still cannot implement the universal quantum computation task. Noting that the wave function $\Psi(\mathbf{v})$ can be calculated in polynomial time under given input values of v_i (see Methods),

and this property also leads to the limitations of the RBM. If a quantum state has a RBM representation, computing $\Psi(\mathbf{v})$ is characterized by the computational complexity class $P/poly$, which represents problems that can be solved by a polynomial-size circuit even if the circuit cannot be constructed efficiently in general. The circuit here denotes the RBM representation $\Psi(\mathbf{v}) = \sum_{\mathbf{h}} e^{E(\mathbf{v}, \mathbf{h})}$, with the input given by a specific \mathbf{v} and the output given by the value of $\Psi(\mathbf{v})$.

The previous art [7] proposed the feature state $|\Phi(\mathbf{x})\rangle = \exp(i \sum_{S \subset [m]} \phi_S(\mathbf{x}) \prod_{i \in S} \sigma_i^z) |0\rangle^m$, and it has been proved that simulating the state $|\Phi(\mathbf{x})\rangle$ in the computational basis is $\#P$ -hard. If the state $|\Phi(\mathbf{x})\rangle$ can be expressed by the RBM, it means $\#P \subset P/poly$ which leads to the polynomial hierarchy collapses. The feature state $|\Phi(\mathbf{x})\rangle$ is one of the instances that the RBM can not simulate efficiently, and other possible examples are projected entangled pair states and the ground states of gapped Hamiltonians. Combining the fact that 2L-QRBM can implement the universal quantum computation task, we successfully illustrate the quantum advantages of 2L-QRBM compared with the RBM.

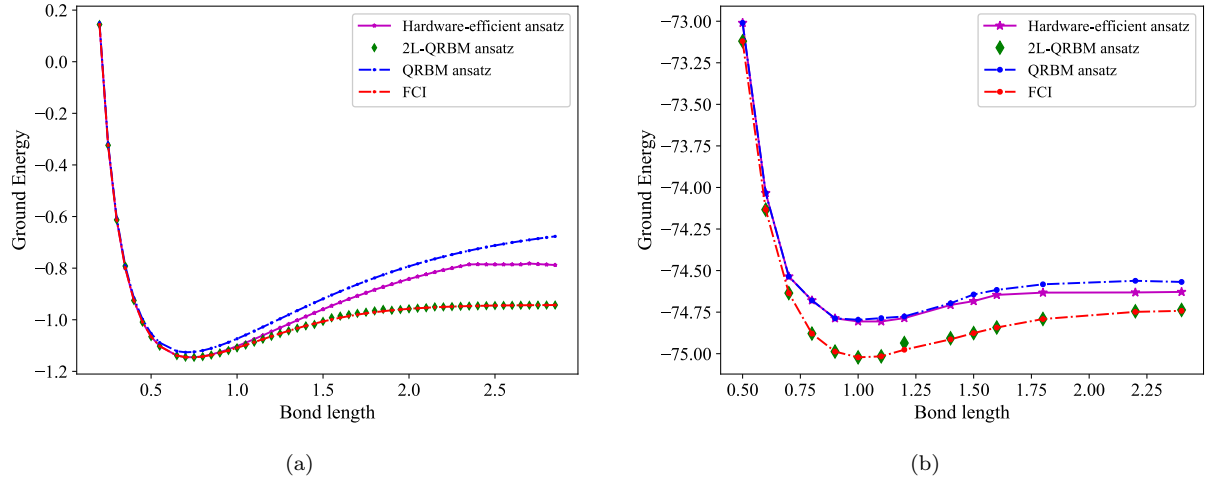


Figure 2: Bond dissociation curves of the Hydrogen molecule (a) and the Water molecule (b). The curves are obtained by repeated computation of the ground state energy for several bond length values. The simulation results are computed by the ProjectQ [27]. (We choose the swap operator as the entanglement operator in the hardware-efficient ansatz.)

Prepare 2L-QRBM by quantum circuit. In this section, we propose an algorithm for preparing the 2L-QRBM by utilizing Quantum Imaginary Time Evolution (QITE) algorithm [24]. Noting that the Hamiltonian $\mathcal{H}_{RBM}(\boldsymbol{\theta}) = \sum_s \hat{h}_s(\boldsymbol{\theta})$ is composed by the linear combination of operators that act on at most k qubits ($k = 1, 2$). According to the Trotter theorem, the operator $e^{\mathcal{H}_{RBM}(\boldsymbol{\theta})}$ can be decomposed as:

$$e^{\mathcal{H}_{RBM}(\boldsymbol{\theta})} = (e^{\Delta\tau \hat{h}_1(\boldsymbol{\theta})} e^{\Delta\tau \hat{h}_2(\boldsymbol{\theta})} \dots)^n + \mathcal{O}(\Delta\tau^2), \quad (6)$$

in which the parameter $n = 1/\Delta\tau$. For the s -term $\hat{h}_s(\boldsymbol{\theta})$, after a single Trotter step, the system becomes to

$$|\Psi\rangle = c^{-1/2} e^{\Delta\tau \hat{h}_s(\boldsymbol{\theta})} |\Psi_0\rangle, \quad (7)$$

and the normalization parameter c can be estimated by $c = 1 - 2\Delta\tau \langle \Psi_0 | \hat{h}_s(\boldsymbol{\theta}) | \Psi_0 \rangle + \mathcal{O}(\Delta\tau^2)$ according to the Taylor approximation. The previous art introduces a unitary operator $e^{-i\Delta\tau A_s(\boldsymbol{\theta})}$ acting on a neighbourhood of the qubits acted on by $\hat{h}_s(\boldsymbol{\theta})$, where the operator $A_s(\boldsymbol{\theta})$ is extended in the Pauli basis $\sigma_{i_1} \dots \sigma_{i_k}$ with relevant parameters $a_s(\boldsymbol{\theta})_{i_1 \dots i_k}$ on k qubits:

$$A_s(\boldsymbol{\theta}) = \sum_{i_1 \dots i_k} a_s(\boldsymbol{\theta})_{i_1 \dots i_k} \sigma_{i_1} \dots \sigma_{i_k}. \quad (8)$$

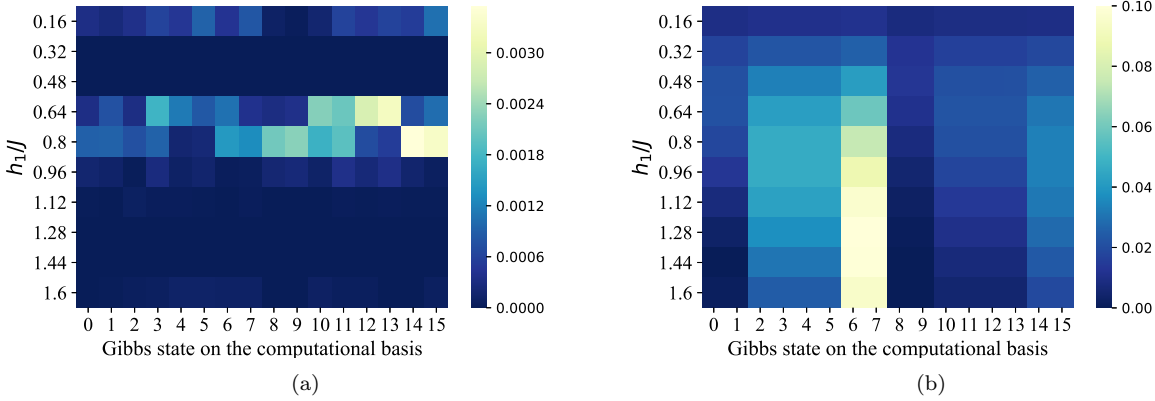


Figure 3: The Gibbs states (thermal states) of the Haldane chain in the case of $N = 9, h_2 = 0, h_1/J \in [0.16, 1.60]$, which are computed by the (a) 2L-QRBM and (b) the hardware-efficient ansatz, respectively. The darker pixels indicate smaller error with the exact value, while the lighter pixels show the opposite. We sample 16 computational basis from the total 512 basis by implementing a large number of measurements (100,000). The simulation error of 2L-QRBM achieves nearly $\epsilon = \mathcal{O}(10^{-4})$.

Define the states $|\Delta_0\rangle = (|\Psi\rangle - |\Psi_0\rangle)/\Delta\tau$ and $|\Delta\rangle = -iA_s(\boldsymbol{\theta})|\Psi_0\rangle$, the goal is to minimize the measurement $\||\Delta_0\rangle - |\Delta\rangle\|$. Taking parameters $a_s(\boldsymbol{\theta})_{i_1 \dots i_k}$ as the variables, this problem can be recognized as an optimization procedure, and parameters $a_s(\boldsymbol{\theta})_{i_1 \dots i_k}$ can be efficiently computed by solving the linear equation

$$(\mathbf{S} + \mathbf{S}^\dagger)\mathbf{a}_s(\boldsymbol{\theta}) = -\mathbf{b}, \quad (9)$$

where the matrix entries $S_{i_1 \dots i_k, j_1 \dots j_k} = \langle \Psi_0 | \sigma_{i_1 \dots i_k}^\dagger \sigma_{j_1 \dots j_k} | \Psi_0 \rangle$ and vector entries $b_{i_1 \dots i_k} = -ic^{-1/2} \langle \Psi_0 | \sigma_{i_1 \dots i_k}^\dagger \hat{h}_s(\boldsymbol{\theta}) | \Psi_0 \rangle$. The entries $S_{i_1 \dots i_k, j_1 \dots j_k}$ and $b_{i_1 \dots i_k}$ all can be efficiently estimated by the swap test method by implementing $\mathcal{O}(1/\epsilon^2)$ measurements with an affordable error ϵ . Although solving the linear function takes the computational overhead $\mathcal{O}(\text{poly}(2^k))$, the k takes values from the set $\{1, 2\}$, then this optimization problem can be efficiently solved by the classical computer once the entries are all obtained.

Experimental results. To solve different tasks, the 2L-QRBM should be trained by different constraints. Given a Hamiltonian $\mathcal{H} = \sum_j \alpha_j P_j$, where $\alpha_j \in \mathcal{R}$ and $P_j = P_j^1 \otimes P_j^2 \otimes \dots \otimes P_j^N, P_j^s \in \{I, X, Y, Z\}$, we here propose two training methods for 2L-QRBM to compute the ground state energy and Gibbs state of \mathcal{H} , respectively.

Compute ground state energy. We first give the elaborate details for training the ansatz to compute the ground state energy. Similar to the variational quantum eigen-solver (VQE) algorithm, the ansatz $|\Psi_v(\boldsymbol{\theta})\rangle$ approximates the ground state along with the energy $E(\boldsymbol{\theta}) = \langle \Psi_v(\boldsymbol{\theta}) | \mathcal{H} | \Psi_v(\boldsymbol{\theta}) \rangle$ is minimized (and meanwhile the Boltzmann parameters theta is trained/updated) by the iterative optimization method. We here utilize a kind of gradient-descent method called “the Simultaneous Perturbation Stochastic Approximation (SPSA) algorithm” to optimize the cost function. SPSA algorithm is robust against the statistical fluctuations, and has shown the merits of high accuracy in the optimization of cost function [5]. Concretely, in every step (e.g. the k -th step) of the SPSA algorithm, the gradient at $\boldsymbol{\theta}_k$ is constructed as $g_k(\boldsymbol{\theta}_k) = (E(\boldsymbol{\theta}^+) - E(\boldsymbol{\theta}^-))\Delta_k/2c_k$, where $\boldsymbol{\theta}_k^\pm = \boldsymbol{\theta}_k \pm c_k \Delta_k$, Δ_k is sampled according to the Bernoulli distribution, and c_k, a_k can be selected with priori experience.

We here simulate the ground state energy of the Hydrogen molecular as well as the Water molecular on ProjectQ, and compares the performance of our 2L-QRBM and previous works including hardware-efficient ansatz [5], QRBM without the transverse field and the Full Configuration Interaction (FCI) method. The numerical results (see Fig.2) shows that, the QRBM without the transverse field and the hardware-efficient ansatz cannot converge to an optimal solution when the bond length increases from 1.5 to 2.5 (both in (a) and (b)), and the curves of our 2L-QRBM are extremely close to that of FCI method.

Compute Gibbs state. We now propose the training method to compute the Gibbs state (thermal state)

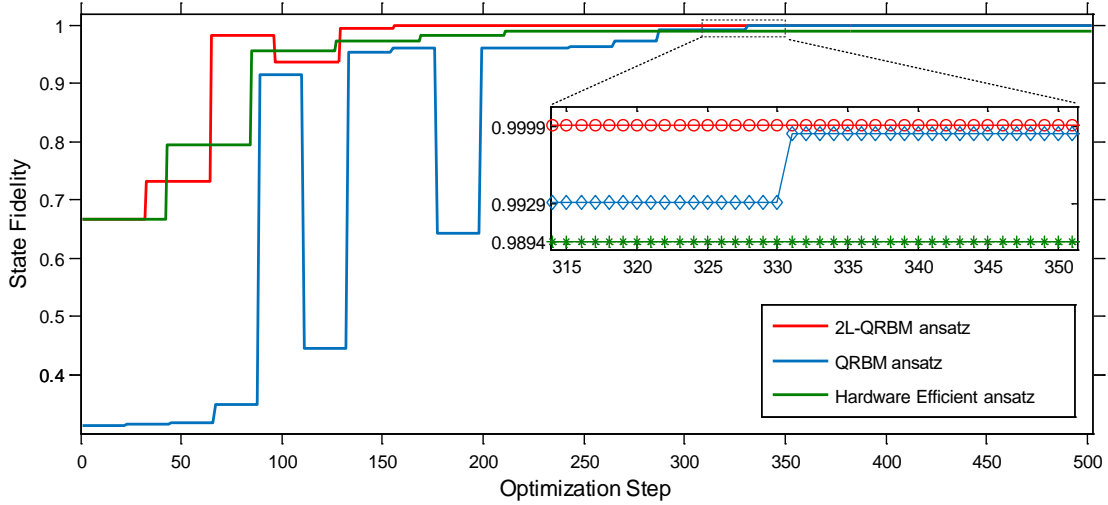


Figure 4: Finding the Gibbs state of Haldane chain with parameters $N = 9, h_1/J = 0.48$ and $h_2 = 0$ by using 2L-QRBM (red line) versus QRBM (blue line) and hardware-efficient ansatz (green line). In this case, the case of 2L-QRBM converges more rapidly to the target state (nearly with the fidelity of 100%) than the other two methods.

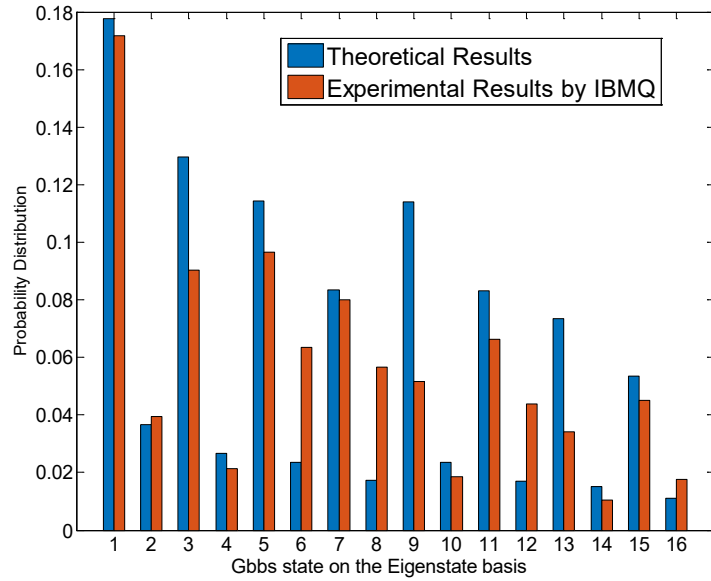


Figure 5: The experimental results by using 2L-QRBM to compute the Gibbs state of Haldane chain on the ibmq-essex chip when $N = 4, h_2 = 0$ and $h_1 = 0.48$. The frequency of the utilized four superconductor qubits are ranging from $[4.4997(GHz), 4.6946(GHz)]$, the maximum error rate of single-qubit-gate is 4.56×10^{-4} , and that for C-NOT gate is 1.474×10^{-2} [28].

$\rho = e^{-\beta \mathcal{H}}/\mathcal{Z}$ of the Hamiltonian $\mathcal{H} = \sum_j \alpha_j P_j$. In general, Gibbs state comes from the process that performing $e^{-\beta \mathcal{H}/2}$ onto the first system of the maximally mixed state $|\phi\rangle = 1/2^{N/2} \sum_x |x\rangle|x\rangle$, followed by tracing out the second system. We here aim to tune the trial state $|\Psi_v(\boldsymbol{\theta})\rangle$ to approximate the state $|\phi_\tau\rangle = c^{-1/2} e^{-\beta \mathcal{H}/2} |\phi\rangle$, where $\tau = 1/\beta$. There might be a doubt why we do not invoke the QITE algorithm to implement $|\phi_\tau\rangle$ directly. Actually, if the target Hamiltonian is k -local (k is not too large), QITE algorithm can efficiently solve the quantum Gibbs sampling problem, otherwise it will induce an enormous computation overhead because it needs to solve a linear function $(\mathbf{S} + \mathbf{S}^\dagger)\mathbf{a}_s(\boldsymbol{\theta}) = -\mathbf{b}$. Fortunately, our 2L-QRBM naturally provides a 2-local Hamiltonian whose ground state can approximate the purified Gibbs state of a k -local Hamiltonian, even when k is large.

We introduce the Wick rotation ($t \rightarrow i\tau$) and the VQE algorithm to adjust the parameter so that the trial state $|\Psi_v(\boldsymbol{\theta})\rangle$ gradually approximates the purified Gibbs state $|\phi_\tau\rangle$. The optimal Boltzmann parameter is obtained when the equation $\delta\|(\partial/\partial\tau + \mathcal{H} - E_\tau)|\Psi_v(\boldsymbol{\theta})\rangle\| = 0$ is satisfied, where E_τ represents the energy term. In this case, the parameter $\boldsymbol{\theta}$ can be obtained from the equation $\theta(\tau + \delta\tau) = \theta(\tau) + A^{-1}(\tau)C(\tau)\delta\tau$, where the elements of matrix A are defined as $A_{mn} = \Re\langle\partial\Psi_v(\boldsymbol{\theta})/\partial\theta_n|\partial\Psi_v(\boldsymbol{\theta})/\partial\theta_m\rangle$, that of C are $C_n = -\Re\langle\partial\theta_n\Psi_v(\boldsymbol{\theta})|\mathcal{H}|\Psi_v(\boldsymbol{\theta})\rangle$ [10]. the notation $\Re(x)$ represents the real part of x .

Following the procedure above, we compute the Gibbs state of a family of Hamiltonians on a spin $-1/2$ chain with the open boundary conditions

$$\mathcal{H} = -J \sum_{i=1}^{N-2} Z_i X_{i+1} Z_{i+2} - h_1 \sum_{i=1}^N X_i - h_2 \sum_{i=1}^{N-1} X_i X_{i+1}, \quad (10)$$

where h_1, h_2 and J are the changeable parameters of the Hamiltonian. We compute the cases that $N = 9, h_2 = 0, h_1/J \in [0.16, 1.60]$ by using the 2L-QRBM ansatz and the hardware-efficient ansatz with swap entanglement operator on the ProjectQ, respectively. We implement 100,000 measurements on the computational basis to reconstruct the target Gibbs state. The results are illustrated as Fig.3 (a) (2L-QRBM) and (b) (hardware-efficient). Each row of the graph represents the amplitude differences $\|P_{trial}(i) - P_{exact}(i)\|$ between the trial state and the target one on the 16 sampled computational bases (from 512 possible basis), where $i \in \{0, 1, \dots, 2^N\}$. Obviously, the error rate induced in 2L-QRBM is nearly $\mathcal{O}(10^{-4})$, which is much less than that of the hardware-efficient ansatz. We also illustrate the optimization steps when computing the Gibbs state of Haldane chain for the specific parameters $N = 9, h_1/J = 0.48$ and $h_2 = 0$ (see Fig.4). It is evident that 2L-QRBM converges to an appropriate destination faster than the other two methods.

Finally, we test the 2L-QRBM model on the IBMQ-essex quantum device by computing the Gibbs state of the Haldane chain (see Fig.5). Limited by the single- and double- gate error rates, the experimental fidelity is only 0.926 which is far below the corresponding theoretical value. We believe that, with the rapidly refinement of the quantum hardware devices, our 2L-QRBM model can simulate much more functions with high accuracy.

Discussion

In summary, we propose a QRBM induced by a specially designed 2-local Hamiltonian, and our model has two salient features, as stated above. First, it is proved that the 2L-QRBM can implement the universal quantum computation tasks, meanwhile our proof implies a new way for understanding the QRBM. Actually, 2L-QRBM can be recognized as the variational version of the QITE algorithm, and this relationship is similar to that for the Quantum Approximation Optimization Algorithm (QAOA) and the Adiabatic Quantum Computation (AQC). We hope our proof can inspire more interesting perspectives on understanding quantum machine learning algorithms in terms of the representational power. Second, our model can be efficiently transformed to the circuit model and be implemented on the NISQ devices. The exact simulation results show the 2L-QRBM trial state can converge to a better solution compared with the widely utilized hardware-efficient ansatz and the Ising model based QRBM. We also test our model on the superconducting quantum devices with 4 qubits, and the experimental results illustrate 2L-QRBM can approximate the target wave function with an acceptable error on the realistic devices. One of the possible reasons for high fidelity performance is that the 2L-QRBM is sufficient for universal quantum computation tasks, therefore the target quantum state is bounded by the Hilbert space that 2L-QRBM can depict. This superior performance shows our model not only has theoretical significance, but also has application values in the NISQ era.

Methods

Review of the RBM. As a classic machine learning technique, the RBM serves as the basis of complex deep learning models such as deep belief networks and deep Boltzmann machines [23]. It comprises a probabilistic network of binary units with a quadratic energy function. The RBM are commonly constituted by one visible layer of N nodes $\mathbf{v} = \{v_i\}_{i=1}^N$, corresponding to the physical spin variables in a chosen basis and a single hidden layer of M auxiliary nodes $\mathbf{h} = \{h_j\}_{j=1}^M$. To maintain consistency with the standard notation in quantum mechanics, the units v_i and h_j take value from $\{0, 1\}$, and the corresponding energy function are identical up to a linear combination of their parameters:

$$E_{\boldsymbol{\theta}}(\mathbf{v}, \mathbf{h}) = \sum_{i=1}^N b_i v_i + \sum_{j=1}^M m_j h_j + \sum_{i=1}^N \sum_{j=1}^M W_{ij} v_i h_j, \quad (11)$$

where $\boldsymbol{\theta} = \{b_i, m_j, W_{ij}\}$ are defined as Boltzmann parameters. The marginal distribution of observing a visible variable \mathbf{v} is given by $\Psi_{\mathbf{v}}(\boldsymbol{\theta}) = \sum_{\mathbf{h}} e^{-E_{\boldsymbol{\theta}}(\mathbf{v}, \mathbf{h})}$ which is an unnormalized probability. Utilizing the RBM to fit a target wave function can be achieved by minimizing the loss function $\mathcal{L}(\boldsymbol{\theta})$ via tuning Boltzmann parameters $\boldsymbol{\theta}$, and the form of $\mathcal{L}(\boldsymbol{\theta})$ depends on the realistic problem.

In the problem of computing the ground state of a Hamiltonian \mathcal{H} , the loss function can be chosen as $\mathcal{L}(\boldsymbol{\theta}) = \langle \Psi(\boldsymbol{\theta}) | \mathcal{H} | \Psi(\boldsymbol{\theta}) \rangle / \langle \Psi(\boldsymbol{\theta}) | \Psi(\boldsymbol{\theta}) \rangle$. The notation $|\Psi(\boldsymbol{\theta})\rangle = \sum_{\mathbf{v}} \Psi_{\mathbf{v}}(\boldsymbol{\theta}) |\mathbf{v}\rangle$ is composed by a series of unnormalized marginal distributions $\Psi_{\mathbf{v}}(\boldsymbol{\theta})$ corresponding to the input basis \mathbf{v} . One needs to compute every amplitudes $\Psi_{\mathbf{v}}(\boldsymbol{\theta})$ according to the input \mathbf{v} with 2^N possibilities, and mediates these amplitudes as the trial state $|\Psi(\boldsymbol{\theta})\rangle$. Then we can utilize optimization algorithms to search an appropriate $\boldsymbol{\theta}^*$ that induces an approximation state $|\Psi(\boldsymbol{\theta}^*)\rangle$ of the target ground state.

To enhance the computational efficiency of the RBM, the QRBM models are proposed. Different from the RBM, the QRBM utilizes a quantum circuit to parallelly compute the amplitudes $\Psi_{\mathbf{v}}(\boldsymbol{\theta})$, and naturally outputs the superposition $|\Psi(\boldsymbol{\theta})\rangle = \sum_{\mathbf{v}} \frac{\Psi_{\mathbf{v}}(\boldsymbol{\theta})}{\mathcal{Z}} |\mathbf{v}\rangle$, where $\mathcal{Z} = \sum_{\mathbf{v}} \Psi_{\mathbf{v}}^2(\boldsymbol{\theta})$ is the normalized factor.

Self energy and effective Hamiltonian. As we concerns only the low energy and ground state of the Hamiltonian, we now illustrate some methods to approximate the Hamiltonian in the low energy space (details refer to [26]).

Given a Hamiltonian H , the Hilbert space \mathcal{H}^{Space} can be divided as $\mathcal{H}^{Space} = \mathcal{L}_+ \oplus \mathcal{L}_-$, where \mathcal{L}_+ is the space spanned by eigenvectors of H with eigenvalues $\lambda \geq \lambda_c$ and \mathcal{L}_- is by that with $\lambda < \lambda_c$. Let Π_{\pm} be the corresponding projection onto \mathcal{L}_{\pm} . Given an operator X on the Hilbert space \mathcal{H}^{Space} , X_{++} is defined as $\Pi_+ X \Pi_+$, which is an operator on \mathcal{L}_+ , and similarly $X_{--} = \Pi_- X \Pi_-$ is an operator on the low energy subspace \mathcal{L}_- .

The self energy of H is defined as

$$\Sigma_-(z) = zI_- - G_{--}^{-1}(z), \quad (12)$$

where $G(z) = (zI - H)^{-1}$. $G(z)$ is a meromorphic operator-valued function of the complex variable z with poles at $z = \lambda_j$, where λ_j is the eigenvalue of H . The self energy $\Sigma_-(z)$ is utilized to approximate the spectrum of H in the low energy subspace. Note that $\Sigma_-(z)$ is nearly constant for a certain range of z , therefore a Hamiltonian \mathcal{H}_{eff} can be selected to approximate it. That is, \mathcal{H}_{eff} can approximate H in the low energy space, so it is generally called “effective Hamiltonian” in the computation of H ’s ground state and ground energy.

The proof of theorem 1.

Theorem 1. *Given a quantum circuit on n -qubits with l -th layer quantum gates implementing a unitary U , suppose $|\alpha(l)\rangle$ is the output of this circuit, then for an arbitrarily small value ϵ there exists a 2-local Hamiltonian \mathcal{H} whose ground state $|\psi\rangle$ is $\mathcal{O}((4/\Delta_{eff} + 1/\sqrt{L})\epsilon)$ close to the state $|\alpha(l)\rangle$, where Δ_{eff} is the gap of the effective Hamiltonian \mathcal{H}_{eff} that approximates the self energy of H .*

We first review several lemmas in [25, 26], which are closely related with our proof of Theorem 1.

Lemma 1 [25]. *Given a quantum circuit on n qubits with L two-qubit gates implementing a unitary U , and $\epsilon > 0$, there exists a 3-local hamiltonian \mathcal{H}_{final} whose ground state is $\mathcal{O}(\epsilon/\sqrt{L})$ close (in trace distance) to the quantum state $U|0\rangle^n$. Moreover, the hamiltonian \mathcal{H}_{final} can be computed by a polynomial time Turing machine.*

Lemma 2[26]. Suppose \mathcal{H} is a Hamiltonian with a spectral gap Δ around the cutoff λ_c (that is, all its eigenvalues are in $(-\infty, \lambda_-] \cup [\lambda_+, +\infty)$, where $\lambda_+ = \lambda_c + \Delta/2$ and $\lambda_- = \lambda_c - \Delta/2$), and V is a Hermite operator with norm $\|V\| \leq \Delta/2$, then for an arbitrary small positive value ϵ , if there exists an operator \mathcal{H}_{eff} whose eigenvalues belongs to $[c, d]$ for some $c < d < \lambda_c - \epsilon$ and moreover, the inequality

$$\|\Sigma_-(z) - \mathcal{H}_{eff}\| \leq \epsilon \quad (13)$$

(where $\Sigma_-(z)$ is the self energy of $\tilde{\mathcal{H}} = \mathcal{H} + V$) holds for all $z \in [c - \epsilon, d + \epsilon]$, each eigenvalue λ_j is ϵ close to the j -th eigenvalue of \mathcal{H}_{eff} .

Lemma 3[26]. Assume that $\mathcal{H}, V, \mathcal{H}_{eff}$ satisfy the conditions of Lemma 2 with some $\epsilon_2 > 0$, let $\lambda_{eff,i}$ denote the i -th eigenvalue of \mathcal{H}_{eff} and $|\tilde{v}\rangle$ (resp., $|v_{eff}\rangle$) denote the ground state of $\tilde{\mathcal{H}}$ (resp., \mathcal{H}_{eff}). Suppose $\lambda_{eff,2}$ and $\lambda_{eff,1}$ are the smallest two eigenvalues of \mathcal{H}_{eff} and $\lambda_{eff,2} > \lambda_{eff,1}$, then we have

$$\|\tilde{v}\rangle - |v_{eff}\rangle\| \leq \frac{2\|V\|^2}{(\lambda_+ - \lambda_{eff,1} - \epsilon_2)^2} + \frac{4\epsilon_2}{\lambda_{eff,2} - \lambda_{eff,1}}. \quad (14)$$

We begin our proof of Theorem 1 now. Given an arbitrary l -layer quantum circuit, without loss of generality, we suppose the input state of this circuit is $|0\rangle^{\otimes n}$ and the output state is quantum state $|\alpha(l)\rangle$. According to Lemma 1, for an arbitrary small positive value ϵ_1 , there exists a 3-local hamiltonian $\mathcal{H}^{(3)}$ whose ground state $|v^{(3)}\rangle$ is $\mathcal{O}(\epsilon_1/\sqrt{L})$ close to $|\alpha(l)\rangle$, that is,

$$\| |v^{(3)}\rangle - |\alpha(l)\rangle \| = \epsilon_1/\sqrt{L}. \quad (15)$$

It is interesting to note that any 3-local Hamiltonian $\mathcal{H}^{(3)}$ can be represented as [26]

$$\mathcal{H}^{(3)} = Y - 6 \sum_{m=1}^M B_{m1} B_{m2} B_{m3}, \quad (16)$$

where Y is a 2-local Hamiltonian with the norm bound $\mathcal{O}(1/n^6)$, $M = \mathcal{O}(n^3)$, n is the scale of the quantum system, and each B_{mi} ($B_{mi} \geq \frac{1}{n^3}I$) is a combination of the Pauli operators. Now we attempt to construct a 2-local Hamiltonian $\mathcal{H}^{(2)}$ whose ground state can approximate that of $\mathcal{H}^{(3)}$. For an arbitrarily small positive value δ , let

$$\mathcal{H} = -\frac{\delta^{-3}}{4} \sum_{m=1}^M I \otimes (\sigma_{m1}^z \sigma_{m2}^z + \sigma_{m1}^z \sigma_{m3}^z + \sigma_{m2}^z \sigma_{m3}^z - 3I), \quad (17)$$

and

$$V = Y \otimes I + \delta^{-1} \sum_{m=1}^M (B_{m1}^2 + B_{m2}^2 + B_{m3}^2) \otimes I - \delta^{-2} \sum_{m=1}^M (B_{m1} \otimes \sigma_{m1}^x + B_{m2} \otimes \sigma_{m2}^x + B_{m3} \otimes \sigma_{m3}^x), \quad (18)$$

then $\mathcal{H}^{(2)} = \mathcal{H} + V$ is a 2-local Hamiltonian, and its self energy can be written as

$$\Sigma_-(z) = Y \otimes I - 6 \sum_{m=1}^M B_{m1} B_{m2} B_{m3} \otimes (\sigma^x)_{eff} + \mathcal{O}(\delta). \quad (19)$$

Let $\mathcal{H}_{eff} = Y \otimes I - 6 \sum_{m=1}^M B_{m1} B_{m2} B_{m3} \otimes (\sigma^x)_{eff}$, the self energy of $\mathcal{H}^{(2)}$ can be rewritten as $\Sigma_-(z) = \mathcal{H}_{eff} + \mathcal{O}(\delta)$. Since $\|\mathcal{H}_{eff}\| \leq \mathcal{O}(1)$ and $\|V\| = \mathcal{O}(\delta^{-2})$, one can apply Lemma 2 with $c = -\|\mathcal{H}_{eff}\|$, $d = \|\mathcal{H}_{eff}\|$, and $\lambda_c = \Delta/2$, where $\Delta = \delta^{-3}$ is the spectral gap of \mathcal{H} . Then we obtain that the smallest eigenvalue of $\mathcal{H}^{(2)}$ is $\mathcal{O}(\delta)$ close to that of \mathcal{H}_{eff} .

We now exploit the relationship between \mathcal{H}_{eff} and $\mathcal{H}^{(3)}$. Note that

$$\mathcal{H}_{eff} = \left(Y - 6 \sum_{m=1}^M B_{m1} B_{m2} B_{m3} \right) \otimes |+\rangle\langle+| + \left(Y + 6 \sum_{m=1}^M B_{m1} B_{m2} B_{m3} \right) \otimes |-\rangle\langle-| \quad (20)$$

$$= \mathcal{H}^{(3)} \otimes |+\rangle\langle+| + \left(Y + 6 \sum_{m=1}^M B_{m1} B_{m2} B_{m3} \right) \otimes |-\rangle\langle-|. \quad (21)$$

and $B_{m1}B_{m2}B_{m3} \geq 0$, then the ground state of \mathcal{H}_{eff} can be written as $|v_{eff}\rangle = |v^{(3)}\rangle|+\rangle$, where $|v^{(3)}\rangle$ is the ground state of $\mathcal{H}^{(3)}$.

Meanwhile, since the 2-local Hamiltonian $\mathcal{H}^{(2)}$, Hermite operator V (Eq.18) and effective Hamiltonian \mathcal{H}_{eff} (Eq.21) satisfy the conditions in Lemma 2, according to Lemma 3, we thus have

$$\| |v^{(2)}\rangle - |v_{eff}\rangle \| \leq \frac{2\|V\|^2}{(\lambda_+ - \lambda_{eff,1} - \epsilon_2)^2} + \frac{4\epsilon_2}{\lambda_{eff,2} - \lambda_{eff,1}}, \quad (22)$$

where $|v^{(2)}\rangle$ is the ground state of $\mathcal{H}^{(2)}$. Since $|v_{eff}\rangle = |v^{(3)}\rangle|+\rangle$ and $\| |v^{(3)}\rangle - |\alpha(l)\rangle \| = \epsilon_1/\sqrt{L}$ (Eq.15), we have:

$$\| |v^{(2)}\rangle - |\alpha(l)\rangle|+\rangle \| \leq \| |v^{(2)}\rangle - |v_{eff}\rangle \| + \| |v_{eff}\rangle - |\alpha(l)\rangle|+\rangle \| \quad (23)$$

$$= \| |v^{(2)}\rangle - |v_{eff}\rangle \| + \| |v^{(3)}\rangle|+\rangle - |\alpha(l)\rangle|+\rangle \| \quad (24)$$

$$\leq \frac{2\|V\|^2}{(\lambda_+ - \lambda_{eff,1} - \epsilon_2)^2} + \frac{4\epsilon_2}{\lambda_{eff,2} - \lambda_{eff,1}} + \frac{\epsilon_1}{\sqrt{L}} = \epsilon(4/\Delta_{eff} + 1/\sqrt{L}) = \mathcal{O}(\epsilon), \quad (25)$$

where $\Delta_{eff} = \lambda_{eff,2} - \lambda_{eff,1}$, $\epsilon = \max\{\epsilon_1, \epsilon_2\} = \mathcal{O}(\delta)$, $\|V\| = \mathcal{O}(\delta^{-2})$, $\lambda_+ = \delta^{-3}$, and $|\lambda_{eff,1}| = \mathcal{O}(1)$.

The proof of theorem 2.

Theorem 2. *For an arbitrary 2-local Hamiltonian \mathcal{H} , there exists a Hamiltonian in the form of*

$$\mathcal{H}_{ax}(\tilde{\theta}) = \sum_{i=1}^N \sum_{t \in \{x,y,z\}} b_i^t v_i^t + \sum_{s=1}^{N-1} \sum_{k=s+1}^N \sum_{t \in \{x,y,z\}} K_{sk}^t v_s^t v_k^t \quad (26)$$

which can approximate \mathcal{H} in the low energy subspace, that is, the Hamiltonian with interaction terms $\sigma_i^s \otimes \sigma_j^l$, $s \neq l \in \{x, y, z\}$ can be approximated by a Hamiltonian with terms $\{\sigma_i^s, \sigma_i^s \otimes \sigma_j^s\}$ in the low energy subspace, where $s \in \{x, y, z\}$.

Proof. Jocob et al.[29] showed that the intersection $\sigma_i^z \sigma_j^x$ can be constructed from $\sigma^x \sigma^x$ and $\sigma^z \sigma^z$. Following their method, we in this section propose how to construct terms $\sigma_i^x \sigma_j^y$ and $\sigma_i^z \sigma_j^y$ by merely using terms $\{\sigma_i^s, \sigma_i^s \otimes \sigma_j^s\}_{i,j=1}^N$, where $s \in \{x, y, z\}$.

Given a 2-local Hamiltonian $\alpha_{ij} \sigma_i^x \sigma_j^y$, our target is to find out a 2-local Hamiltonian $\mathcal{H}^{(2)}$, which is composed by $\sigma^x, \sigma^y, \sigma^x \sigma^x$ and $\sigma^y \sigma^y$, to approximate $\alpha_{ij} \sigma_i^x \sigma_j^y$ in the low energy subspace. Without loss of generality, suppose $\mathcal{H}^{(2)} = h_i \sigma_i^x + h_j \sigma_j^x + \Delta_i \sigma_i^y + \Delta_j \sigma_j^y + J_{ij} \sigma_i^x \sigma_j^x + K_{ij} \sigma_i^y \sigma_j^y$, in which $(h_i, h_j, \Delta_i, \Delta_j, J_{ij}, K_{ij})$ are real-valued parameters to be confirmed. We will find out an appropriate parameters $(h_i, h_j, \Delta_i, \Delta_j, J_{ij}, K_{ij})$ to construct a $\mathcal{H}^{(2)}$ that can approximate $\alpha_{ij} \sigma_i^x \sigma_j^y$ in the low energy subspace. The elaborate procedure is illustrated as follows.

We first consider a perturbation Hermite operator $V = V_1 + V_2 + V_3$:

$$V_1 = (\mathcal{H}^{(2)} + D(\sigma_j^y + I)) \otimes I_k - A \sigma_i^x \otimes |-\rangle\langle-|_k, \quad (27)$$

$$V_2 = B(\sigma_j^y \otimes I) \otimes \sigma_k^y, \quad (28)$$

and

$$V_3 = C \sigma_i^x \otimes |+\rangle\langle+|_k, \quad (29)$$

where A, B, C, D are also the real-valued parameters to be confirmed later. Then, the self energy operator $\Sigma_-(z)$ of the 2-local Hamiltonian $(\mathcal{H}^{(2)} + V)$ can be expressed by

$$\Sigma_-(z) = \tilde{\mathcal{H}}^{(2)} + \left(\frac{2B^2C}{(z - \delta^{-1})^2} - A \right) \sigma_i^x + \left(\frac{2B^2}{z - \delta^{-1}} + D + \frac{4DB^2}{(z - \delta^{-1})^2} \right) (\sigma_j^y + I) + \frac{2B^2C}{(z - \delta^{-1})^2} \sigma_i^x \sigma_j^y + \mathcal{O}(\delta^3), \quad (30)$$

in which δ is an arbitrary small value, and $\tilde{\mathcal{H}}^{(2)} = \mathcal{H}^{(2)} + \frac{B^2}{(z-\delta^{-1})^2}(\sigma_j^y + I)\mathcal{H}^{(2)}(\sigma_j^y + I)$. Now we can replace the coupling strengths $(h_i, h_j, \Delta_i, \Delta_j, J_{ij}, K_{ij})$ by:

$$h_i \mapsto h_i \left(1 + \frac{2B^2}{(z-\delta^{-1})^2} \right), \quad (31)$$

$$\Delta_i \mapsto \Delta_i \left(1 + \frac{2B^2}{(z-\delta^{-1})^2} \right) + \frac{2B^2}{(z-\delta^{-1})^2} K_{ij}, \quad (32)$$

$$\Delta_j \mapsto \Delta_j \left(1 + \frac{2B^2}{(z-\delta^{-1})^2} \right), \quad (33)$$

$$K_{ij} \mapsto K_{ij} \left(1 + \frac{2B^2}{(z-\delta^{-1})^2} \right) + \frac{2B^2}{(z-\delta^{-1})^2} \Delta_i, \quad (34)$$

and choose the parameters $A = \alpha_{ij}, B = (1/\delta E)^{2/3}E, C = \alpha_{ij}(1/\delta E)^{2/3}/2$ and $D = 2\delta^{-1/3}E^{2/3}$, where E is a constant parameter. Then the self-energy can be simplified as:

$$\Sigma(0)_- = \tilde{\mathcal{H}}^{(2)} + \alpha_{ij}\sigma_i^x\sigma_j^y + \mathcal{O}(\delta^3). \quad (35)$$

Since $\Sigma(0)_-$ is a decent approximation of $\mathcal{H}^{(2)}$ in the low energy subspace, and the ground state of $\Sigma(0)_-$ is extremely close to that of $\tilde{\mathcal{H}}^{(2)} + \alpha_{ij}\sigma_i^x\sigma_j^y$, then the ground state of $\alpha_{ij}\sigma_i^x\sigma_j^y$ is extremely close to that of the Hamiltonian $(\mathcal{H}^{(2)} - \tilde{\mathcal{H}}^{(2)})$ which is only composed by $\sigma^x, \sigma^y, \sigma^x\sigma^x$ and $\sigma^y\sigma^y$.

The method for constructing $\sigma^y\sigma^z$ is similar to the procedure above.

The proof of theorem 3.

Theorem 3. *Given a 2-local $2^n \times 2^n$ Hamiltonian $\mathcal{H} = \sum_j \alpha_j P_j$, in which parameters $\vec{\alpha} = (\alpha_1, \alpha_2, \dots) \in \mathcal{R}^{poly(n)}$ and $P_j \in \{\sigma_i^s, \sigma_i^s \otimes \sigma_j^s\}_{i,j=1}^n$, the ground state $|\psi_0\rangle$ of \mathcal{H} can be approximated by the 2L-QRBM trial state $|\Psi(\theta^*)\rangle$ with the fidelity of $(1 - \mathcal{O}(\epsilon))$ when the Boltzmann parameter $\theta^* = \{m_j, W_{i1}, b_i^t, K_{sk}^t\} = \{0, \ln(e^{\lambda^*\tau/n} + \sqrt{e^{2\lambda^*\tau/n} - 1}), -\tau\vec{\alpha}\}$. The parameter $\lambda^* > 0$ is the ‘phase shift’ and $\tau = \mathcal{O}((\log 1/\epsilon + n))$, where ϵ is the error provided by the truncated terms.*

Proof: Since the Hamiltonian \mathcal{H} is a Hermite matrix, then it can be expressed as the spectrum decomposition:

$$\mathcal{H} = \sum_{j=0}^{2^n-1} E_j |\psi_j\rangle\langle\psi_j|, \quad (36)$$

where E_j is the j -th eigenvalue whose corresponding eigenvector is $|\psi_j\rangle$. Without loss of generality, suppose the eigenvalues $\{E_j\}$ is an increasing sequence, that is, $E_0 < E_1 < \dots < E_{2^n-1}$, then E_0 represents the ground state energy and $|\psi_0\rangle$ represents the ground state of the Hamiltonian \mathcal{H} . According to Eq.(36), the Hamiltonian $\tilde{\mathcal{H}} = \mathcal{H} - E_0 \cdot I$ has the same eigenvectors to that of \mathcal{H} and its eigenvalues $\tilde{E}_j = E_j - E_0$ are all non-negative.

We first introduce the ‘phase shift’ value λ^* satisfying $\tilde{E}_0 < \lambda^* \leq \tilde{E}_1$. This value can be estimated in advance by for example the phase estimation algorithm or VQE algorithm. Let

$$\mathcal{H}^* = \tilde{\mathcal{H}} - \lambda^* I = \sum_{j=0}^{2^n-1} (\tilde{E}_j - \lambda^*) |\psi_j\rangle\langle\psi_j|. \quad (37)$$

and $E_j^* = \tilde{E}_j - \lambda^*$, then we have $E_0^* < 0, E_j^* \geq 0$ for $j = 1, \dots, 2^n - 1$, and the ‘phase shift’ $\lambda^* > 0$.

For the 2L-QRBM with $M = 1$ and $\theta^* = \{m_j, W_{i1}, b_i^t, K_{sk}^t\} = \{0, W_{i1}, -\tau\vec{\alpha}\}$, the trial state of it can be expressed as

$$|\Psi_v(\theta)\rangle = \frac{c^{-1/2}}{2^n} \prod_{i=1}^n (e^{W_{i,1}} + e^{-W_{i,1}}) \exp(\mathcal{H}_{ax}(-\tau\vec{\alpha})) |+\rangle_v^{\otimes n}. \quad (38)$$

Let the interaction weights $W_{i1} = \ln(e^{\lambda^* \tau/n} + \sqrt{e^{2\lambda^* \tau/n} - 1})$ and note that $\mathcal{H}_{ax}(-\tau \vec{\alpha}) = -\tau \mathcal{H}$, then we have

$$|\Psi_v(\boldsymbol{\theta})\rangle = c^{-1/2} \exp(\lambda^* \tau I) \exp(-\tau \mathcal{H}) |+\rangle_v^{\otimes n} = c^{-1/2} e^{-\tau(\mathcal{H} - \lambda^* I)} |+\rangle_v^{\otimes n}. \quad (39)$$

Suppose the initial state $|+\rangle_v^{\otimes n}$ of the 2L-QRBM has the overlap K with the ground state, then

$$|\Psi_v(\boldsymbol{\theta})\rangle = \frac{Ke^{-(E_0 - \lambda^*)\tau}}{\sqrt{c}} |\psi_0\rangle + \sqrt{1 - \frac{K^2 e^{-2(E_0 - \lambda^*)\tau}}{c}} |\psi_0^\perp\rangle. \quad (40)$$

The state $|\psi_0^\perp\rangle$ is composed by the eigenstates $|\psi_1\rangle, \dots, |\psi_{2^n-1}\rangle$ that are orthogonal to $|\psi_0\rangle$:

$$|\psi_0^\perp\rangle = \sum_{j=1}^{2^n-1} a_j e^{-(E_j - \lambda^*)\tau} |\psi_j\rangle, \quad (41)$$

where $a_j \in \mathcal{C}$ are the complex parameters. Since $E_0 - \lambda^* < 0$ and $E_j - \lambda^* \geq 0, j = 1, \dots, 2^n - 1$, the amplitudes $a_j e^{-(E_j - \lambda^*)\tau}$ will converge to 0 rapidly with the increase of τ , and meanwhile $\frac{Ke^{-(E_0 - \lambda^*)\tau}}{\sqrt{c}}$ will increase to nearly 1 [15]. Then the overlap (fidelity) between 2L-QRBM $|\Psi_v(\boldsymbol{\theta})\rangle$ and the ground state $|\psi_0\rangle$ can be estimated by

$$F(|\Psi_v(\boldsymbol{\theta})\rangle, \psi_0) = \frac{K^2 e^{-2(E_0 - \lambda^*)\tau}}{K^2 e^{-2(E_0 - \lambda^*)\tau} + \sum_j \|a_j\|^2 e^{-2(E_j - \lambda^*)\tau}} \quad (42)$$

$$= 1 - \frac{\epsilon}{e^{-2(E_0 - \lambda^*)\tau} + \epsilon}, \quad (43)$$

where ϵ represents the truncated terms $\sum_j \|a_j\|^2 e^{-2(E_j - \lambda^*)\tau}$ converging to 0 when the parameter $\tau = \mathcal{O}((\log 1/\epsilon + n)/\min\{E_j - \lambda^*\})$.

Quantum advantages of 2L-QRBM. The classical analogue of 2L-QRBM is the modified restricted Boltzmann machine with connection of two visible nodes, and its wave function can be described as $\Psi(\mathbf{v}) = \sum_{\mathbf{h}} e^{E(\mathbf{v}, \mathbf{h})}$, where the energy function

$$E(\mathbf{v}, \mathbf{h}) = \sum_i b_i v_i + \sum_j m_j h_j + \sum_{ij} W_{ij} v_i h_j + \sum_{i,j} K_{ij} v_i v_j. \quad (44)$$

It is interesting to note that the marginal distribution $\Psi(\mathbf{v})$ can be computed as

$$\Psi(\mathbf{v}) = \exp \left(\sum_i b_i v_i + \sum_{i,j} K_{ij} v_i v_j \right) \prod_{j=1}^M \cosh \left(m_j + \sum_i W_{ij} v_i \right), \quad (45)$$

which means the wave function $\Psi(\mathbf{v})$ can be calculated in polynomial time under given input values to the variables v_i . And this property also leads to the limitations of the modified RBM. If a quantum state has a modified RBM representation, computing $\Psi(\mathbf{v})$ is characterized by the computational complexity class P/poly which represents problems that can be solved by a polynomial-size circuit even if the circuit cannot be constructed efficiently in general. The circuit here denotes the modified RBM representation, with the input given by a specific \mathbf{v} and the output given by the value of $\Psi(\mathbf{v})$.

The previous arts [7] proposed the feature state $|\Phi(\mathbf{x})\rangle = \exp(i \sum_{S \subset [m]} \phi_S(\mathbf{x}) \prod_{i \in S} \sigma_i^z) |0\rangle^m$ which is proved $\#P$ -hard for classical computer. If the state $|\Phi(\mathbf{x})\rangle$ can be expressed by the modified RBM, it means $\#P \subset P/\text{poly}$ which leads to the polynomial hierarchy collapses. The feature state $|\Phi(\mathbf{x})\rangle$ is one of the instances that modified RBM can not simulate efficiently, and other possible examples are projected entangled pair states and the ground states of gapped Hamiltonians. Combining the above theorems 1 and 2, we successfully illustrate the quantum advantages of 2L-QRBM in terms of the representation power.

References

1. R. P. Feynman, Simulating physics with computers, *International journal of theoretical physics* 21.6, 133-153, (1999).
2. Abrams, D, Seth Lloyd, Simulation of many-body Fermi systems on a universal quantum computer. *Phys. Rev. Lett.* 79, 2586-2589, (1997)
3. Aspuru-Guzik, et al., Simulated quantum computation of molecular energies. *Science* 309, 1704-1707, (2005).
4. A. Peruzzo, J. McClean, P. Shadbolt, Man-Hong Yung, X. Zhou, P. J. Love, A. Aspuru-Guzik, and J. L. O'Brien, A variational eigenvalue solver on a photonic quantum processor. *Nat. Commun.* 5, 4213, (2014).
5. A. Kandala, A. Mezzacapo, K. Temme, M. Takita, M. Brink, J. M. Chow, and J. M. Gambetta, Hardware-efficient variational quantum eigensolver for small molecules and quantum magnets. *Nature* 549, 242-246, (2017).
6. Carleo, G. and Troyer, M. Solving the quantum many-body problem with artificial neural networks. *Science* 355, 602-606, (2017).
7. V. Havlicek, A. Corcoles, K. Temme, A. W. Harrow, A. Kandala, J. M. Chow and J. M. Gambetta. Supervised learning with quantum-enhanced feature spaces. *Nature* 567, 209-212, (2019).
8. Xun Gao and Lu-Ming Duan, Efficient representation of quantum many-body states with deep neural networks. *Nat. Commun.* 8, 662, (2017).
9. B. Kulchytskyy, E. Andriyash, M. Amin, and R. Melko. Quantum boltzmann machine. *Phys. Rev. X* 33, 489-493, (2016).
10. S. McArdle, T. Jones, S. Endo, L. Ying, C. B. Simon and X. Yuan, Variational ansatz-based quantum simulation of imaginary time evolution. *npj Quantum Inf* 5, 75, (2019).
11. Rongxin Xia, and Sabre Kais, Quantum machine learning for electronic structure calculations, *Nat. Commun.* 9, 4195, (2018).
12. Chang Yu Hsieh, Qiming Sun, Shengyu Zhang, and Chee Kong Lee, Unitary-Coupled Restricted Boltzmann Machine Ansatz for Quantum Simulations, *arXiv:1912.02988*, (2019).
13. Choo, K., Mezzacapo, A. and Carleo, G. Fermionic neural-network states for ab-initio electronic structure. *Nat. Commun.* 11, 2368, (2020).
14. Yusen Wu, Chao-hua Yu, Sujuan Qin, Qiaoyan Wen, and Fei Gao, Bayesian machine learning for Boltzmann machine in quantum-enhanced feature spaces, *arXiv:1912.10857*, (2019).
15. Lehtovaara, L., Toivanen, J. and Eloranta, J. Solution of time-independent schrodinger equation by the imaginary time propagation method. *J. Comput. Phys.* 221, 148-157, (2007).
16. W. A. Harrow, A. Hassidim, and S. Lloyd. Quantum algorithm for linear systems of equations. *Phys. Rev. lett.* 103, 150502, (2009).
17. Chao-hua Yu, Fei Gao, et al. Quantum algorithm for visual tracking. *Phys. Rev. A* 99, 022301, (2019).
18. Chao-hua Yu, Fei Gao, and Qiaoyan Wen, Quantum algorithms for ridge regression. *IEEE Transactions on Knowledge and Data Engineering (TKDE)* 29, 37491, (2019).
19. Linchun Wan, Chao-hua Yu, Shijie Pan, Fei Gao, Qiaoyan Wen, and Sujuan Qin. Asymptotic quantum algorithm for the toeplitz systems. *Phys. Rev. A* 97.6, (2018).
20. Yusen Wu et al. Quantum conditional random field. *arXiv:1901.01027*, (2019).

21. P.Wittek and S.Lloyd. Quantum machine learning. *Nature*, 549, 195, (2017).
22. Roger G. Melko, Giuseppe Carleo, Juan Carrasquilla and J. Ignacio Cirac. Restricted Boltzmann machines in quantum physics. *Nat. Phys.* 15, 887-892, (2019).
23. G. E. Hinton, R. R. Salakhutdinov. Reducing the Dimensionality of Data with Neural Networks. *Science*, 313, (2006)
24. Mario Motta, Chong Sun, Adrian T.K.Tan, Matthew J.O.Rourke, Erika Ye, Austin J. Minnich, Fernando G.S.L.Brandao, and Garnet Kin-Lic Chan, Determining eigenstates and thermal states on a quantum computer using quantum imaginary time evolution, *Nat. Phys.* 16, 1-6, (2019).
25. Dorit Aharonov, Wim van Dam, Julia Kempe, Zeph Landau, Seth Lloyd, and Oded Regev, Adiabatic Quantum Computation is Equivalent to Standard Quantum Computation, *SIAM J. Comput.* 37, 166-194,(2005).
26. Julia Kempe, Alexei Kitaev, and Oded Regev, The Complexity of the Local Hamiltonian Problem, *SIAM J. Comput.* 35, 1070-1097, (2006).
27. Damian S. Steiger, Matthias Troyer et al., ProjectQ: An Open Source Software Framework for Quantum Computing, *Quantum* 2, 49, (2018).
28. IBM Qiskit group, Abraham et al., Qiskit: An Open-source Framework for Quantum Computing, 10.5281/zenodo.2562110, (2019).
29. Jacob D. Biamonte and Peter J. Love, Realizable Hamiltonians for universal adiabatic quantum computers, *Phys. Rev. A* 78, 012352, (2008).

Acknowledgments

This work is supported by NSFC (Grant Nos. 61976024, 61972048), and the Fundamental Research Funds for the Central Universities (Grant No.2019XD-A01).

Author contributions

All authors contributed extensively to the work presented in this paper.